(12) LEVEL III

AD-E430515

AD

TECHNICAL REPORT ARBRL-TR-02258

BRLGRAY: THE BALLISTIC RESEARCH LABORATORY VERSION OF THE GRAY EQUATION OF STATE

Joseph F. Lacetera

August 1980

US ARMY ARMAMENT RESEARCH AND DEVELOPMENT COMMAND
BALLISTIC RESEARCH LABORATORY
ABERDEEN PROVING GROUND, MARYLAND

UNCLASSIFIED
SECURITY CLASSIFICATION OF THIS PAGE (When Data Entered)

REPORT DOCUMENTATION PAGE

READ INSTRUCTIONS
BEFORE COMPLETING FORM

1. REPORT NUMBER
TECHNICAL REPORT ARBRL-TR- 02258

2. GOVT ACCESSION NO.
AD-A091246

3. RECIPIENT'S CATALOG NUMBER

4. TITLE (and Subtitle)
BRLGRAY: The Ballistic Research Laboratory
Version of the Gray Equation of State

5. TYPE OF REPORT & PERIOD COVERED

6. PERFORMING ORG. REPORT NUMBER

7. AUTHOR(s)
Joseph F. Lacetera

8. CONTRACT OR GRANT NUMBER(s)

9. PERFORMING ORGANIZATION NAME AND ADDRESS
US Army Ballistic Research Laboratory
ATTN: DRDAR-BLB
Aberdeen Proving Ground, MD 21005

10. PROGRAM ELEMENT, PROJECT, TASK AREA & WORK UNIT NUMBERS
RDT&E 1L161102AH43

11. CONTROLLING OFFICE NAME AND ADDRESS
USA Armament Research & Development Command
Ballistic Research Laboratory (ATTN: DRDAR-BL)
Aberdeen Proving Ground, MD 21005

12. REPORT DATE
AUGUST 1980

13. NUMBER OF PAGES
40

14. MONITORING AGENCY NAME & ADDRESS(if different from Controlling Office)

15. SECURITY CLASS. (of this report)
UNCLASSIFIED

15a. DECLASSIFICATION/DOWNGRADING SCHEDULE

16. DISTRIBUTION STATEMENT (of this Report)

Approved for public release; distribution unlimited.

17. DISTRIBUTION STATEMENT (of the abstract entered in Block 20, if different from Report)

18. SUPPLEMENTARY NOTES

19. KEY WORDS (Continue on reverse side if necessary and identify by block number)

Equation of State	GRAY	BRLGRAY
Three-Phase	Metals	Liquid-Vapor
Melt	Solid-Liquid	Grover Scaling Law
Young-Alder	HELP Code	Hydrocode
Tillotson	Hull Code	

20. ABSTRACT (Continue on reverse side if necessary and identify by block number)

The BRLGRAY EOS is described. EOS input parameters and mixed-phase boundaries are shown for Al, Cu, and Fe. Comparisons are shown with Tillotson and HULL EOS's.

DD FORM 1 JAN 73 1473 EDITION OF 1 NOV 65 IS OBSOLETE

UNCLASSIFIED
SECURITY CLASSIFICATION OF THIS PAGE (When Data Entered)

TABLE OF CONTENTS

LIST OF FIGURES

LIST OF TABLES

1. BACKGROUND

A. HISTORICAL DEVELOPMENT OF GRAY EOS

The original GRAY three-phase equation of state (EOS) for metals was developed by Royce[1] at the Lawrence Livermore Laboratory(LLL). It included a Gruneisen description of the solid referenced to the solid Hugoniot[2], and a scaling law EOS for liquid developed by Grover[3]. Material in the liquid-vapor region was described by a classical hard-sphere EOS due to Young and Alder[4] which included a van der Waals attractive term.

The solid-liquid model assumed: the entropy of the melting is independent of pressure; the temperature dependence of the specific heat in the liquid is a universal curve scaled on the melting temperature; and the pressure dependence of the melting temperature is given by a modified Lindemann law.

The Grover scaling law and the Young-Alder model were analytically joined at a volume in the range 1.3 to 1.5 times the normal volume by adding correction terms to the Young-Alder model at the low density side of the join volume.

Young[5] subsequently introduced a modification of the original GRAY EOS to permit the calculation of the pressure in the mixed-phase liquid-vapor region; however the basic physical models and join procedure were not altered.

A substantially modified GRAY EOS, BRLGRAY, was developed in 1976 under Ballistic Research Laboratory (BRL) sponsorship by Wray[6] at Systems, Science and Software. Modifications included a continuous model for the liquid phase, a soft-sphere model for the vapor region, and an improved join procedure for the liquid and vapor regions.

---

[1] *E.B. Royce, "GRAY, A Three-Phase Equation of State for Metals", Lawrence Livermore Laboratory, UCRL-51121, Sep 1971.*

[2] *R. N. Keeler and E. B. Royce, "Shock Waves in Condensed Media", Lawrence Livermore Laboratory, UCRL-71846, 1969.*

[3] *R. Grover, "Liquid Metal Equation of State Based on Scaling", J. Chem Phys, 55, 3435, 1971.*

[4] *D. A. Young and B. J. Alder, "Critical Point of Metals from the van der Waals Model", Phys Rev A3, 364, 1971.*

[5] *D. A. Young, "Modification of the GRAY Equation of State in the Liquid-Vapor Region" Lawrence Livermore Laboratory, UCRL-51575, Apr 15, 1974.*

[6] *William O. Wray and Robert A. Cecil, "Modified GRAY: An Improved Three-Phase Equation of State for Metals". BRL CR No. 299, April 1976.* (AD #A025260)

The fluid (liquid and gas) models share a single continuous representation of the specific heat. This eliminates the artificial hot liquid region of the original model. The soft sphere representation in the vapor region yields a model which is physically realistic at higher temperatures and more compatible with the Grover model.

B. APPLICATIONS

Multi-phase EOS's are required for the numerical modelling of the response of materials to dynamic loading under which solid phase changes, melt transitions, and vapor states occur. However, equations of state currently in use for such problems include the Tillotson EOS[7] which is used in the hydrocode HELP75[8] , and curve fits such as that used in the HULL[9] code. These EOS's do not take into account phase changes which may be important in calculating material response to dynamic loading.

HELP75 is the most recent documented version of the HELP code. However, it does not calculate internal energy accurately and therefore cannot properly predict thermodynamic state. HULL is an Eulerian code which uses a curve fit to EOS data, but it uses the same type of energy calculation as does HELP75.

BRLHELP[10] is a new improved version of HELP. It has a modification due to Schmitt[11] which enables it to calculate internal energies very accurately, has improved input formatting[12] and in its latest version has the BRLGRAY EOS for metals.

Janet Lacetera[13] has done parameter studies, using the HELP code, for a variety

---

[7] *J. H. Tillotson, "Metal Equations of State for Hypervelocity Impact", General Atomic Report GA-3216, July 1962.*

[8] *Laura J. Hageman, et al, "HELP, a Multi-Material Eulerian Program for Compressible Fluid and Elastic-Plastic Flows in Two Space Dimensions and Time", Systems, Science, and Software Report TR-76-45-BK2, Apr 1976.*

[9] *Richard E. Durrett and David A. Matuska, "The HULL Code, A Finite Difference Solution to the Equations of Continuum Mechanics", Air Force Armament Laboratory, AFATL-TR-78-125, Nov 1978.*

[10] *J. Lacetera, J. E. Lacetera, and J. A. Schmitt, "The BRL 7600 Version of the HELP Code", BRL REPORT ARBRL-TR-02209, Jan 80.* (AD #A082804)

[11] *J. A. Schmitt, "An Improved Internal Energy Calculation for the HELP Code and Its Implications to Conical Shaped Charge Simulations", BRL Report ARBRL-TR-02168, Jun 79.* (AD #A072785)

[12] *J. Lacetera, "BRLHELP80: NAMELIST INPUT", BRL IMR No 677, Mar 80.*

[13] *Janet Lacetera, "Study of Liner Collapse and Jet Formation for Various Hemispherical Shaped-Charge Designs", BRL Draft Report.*

of problems. Agreement with experiment for these calculations has been quite good and indicates that the HELP code provides sufficiently accurate information to be used as a design optimization tool in hydrocode applications. However, the EOS imbedded in the code does not adequately represent the effects of phase changes. For applications where such phenomena are important a more sophisticated EOS is appropriate.

We have made comparisons between BRLGRAY, Tillotson, and the HULL EOS's. In the solid state the agreement between these EOS's and with experiment is excellent. Significantly, BRLGRAY uses no more computer time than do the others for solid state calculations and outperforms the others in the melt transition and at higher temperatures. A comparison of the BRLGRAY EOS and that used in the HULL code, for temperature as a function of energy for copper, is shown in Figure 1. The phase transition, in BRLGRAY, begins at an energy of 4.62 ergs/g and is complete at an energy of 6.67 ergs/g. This heat of transition of 2.05 ergs/g is very close to the values given in the various handbooks. Figure 2 is another illustration of the BRLGRAY melt-phase transition: ambient-pressure temperature profiles are shown for the copper and aluminum. The melt temperatures are 1356 K for copper and 932 K for aluminum. The melt transition is simply not calculated by the other EOS's.

2. The BRLGRAY Equation of State*

A. Solid Region

This portion of the EOS remains unmodified. Grover's scaling law includes a Gruneisen description of the solid referenced to the experimental Hugoniot. The volume dependence of gamma in the solid is linear. Energy and pressure in this region are given by

$$E_s(T,V) = E_o(V) + 3R' + \frac{G'T^2}{2}, \tag{1}$$

and

$$P_s(T,V) = P_o(V) + 3\gamma_s(V)\frac{R'T}{V} + \frac{1}{2}\gamma_e\frac{G'T^2}{V}, \tag{2}$$

where R' and G' are the atomic-weight scaled gas constant and electronic energy coefficient respectively, Po(V) and Eo(V) are reference values at 0° K, and $\gamma_s(V)$ is the volume-dependent Gruneisen coefficient for the solid.

---

* *A list of symbols for the EOS is given in Appendix A, and a complete list of the EOS equations is given in Appendix B.*

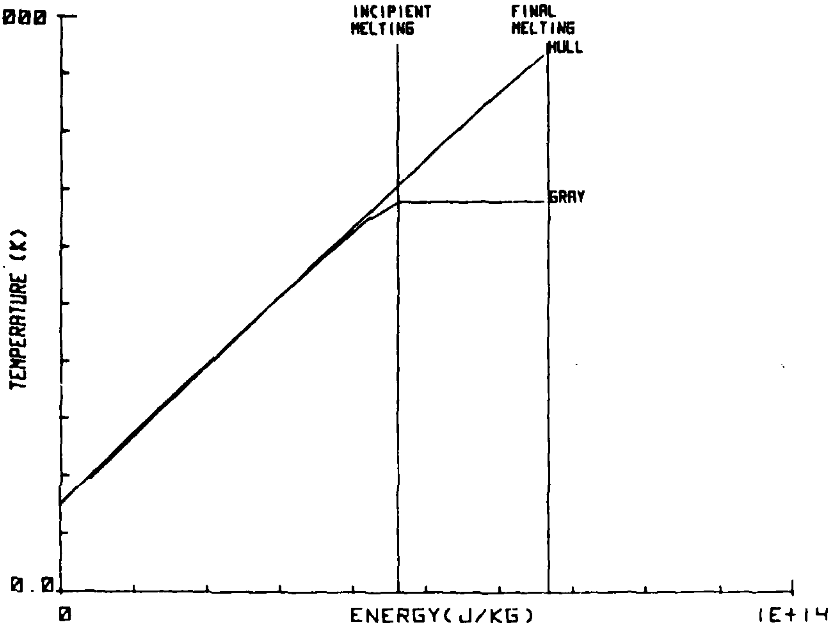

FIGURE 1. TEMPERATURE VS ENERGY; GRAY VS HULL

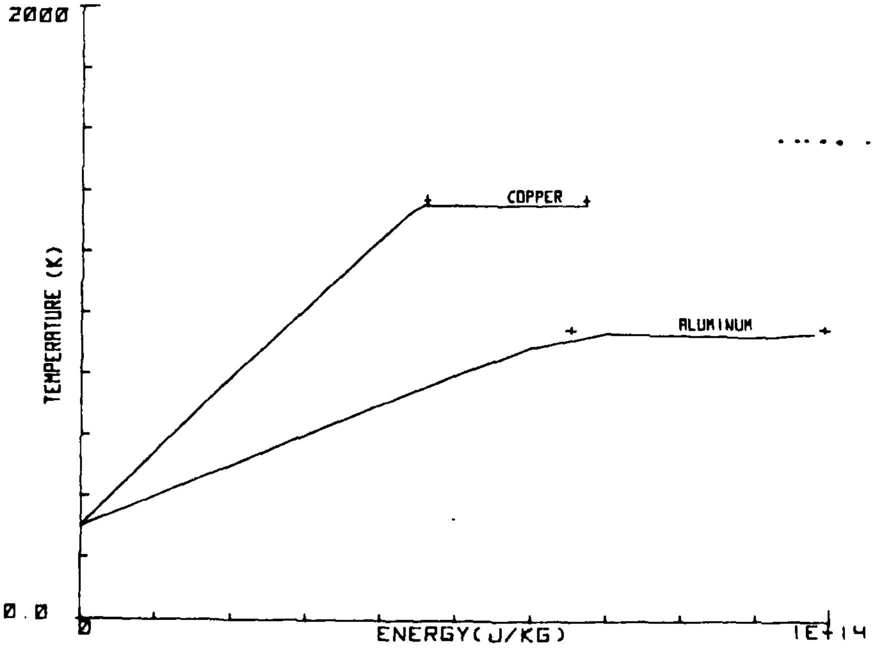

FIGURE 2. AMBIENT PRESSURE TEMPERATURES

The atomic-weight scaled electronic energy coefficient is given by

$$G' = \frac{\pi^2 N_e k R'}{2E_f}, \tag{3}$$

where the Fermi energy, E_f is given by

$$E_f = 26\left[\frac{N_e}{WV_o}\right]^{2/3}, \tag{4}$$

where W is atomic weight, and N_e is number of free electrons.

The complete solid EOS is described by Royce[1]. The experimental Hugoniot is assumed to have the standard form:

$$U_s = C + SU_p, \tag{5}$$

$$P_H(V) = \frac{\rho_o C^2 x}{(1-Sx)^2}, \tag{6}$$

and

$$E_H(V) = \frac{1}{2}P_H(V)[V_o-V] + E_{oH}, \tag{7}$$

where x is a compression variable, and C and S are Hugoniot parameters. To reference the EOS to the Hugoniot, $\Gamma(T,V)$ is defined by the the Gruneisen- like equation

$$P(T,V) = P_o(V) + \frac{\Gamma(T,V)}{V}\Big[E(T,V) - E_o(V)\Big], \tag{8}$$

and the Hugoniot in the solid is written

$$P_H = P_o(V) + \frac{\gamma_s(V)}{V}\Big[E_H(V) - E_o(V)\Big], \tag{9}$$

where γ_s is the volume-dependent Gruneisen parameter in the solid.

Equations 7-9 are combined, using $\Gamma(T=0,V)=\gamma_s(V)$ to give

$$\begin{aligned} P(T,V) = P_H(V)[1 - \frac{\gamma_s(V)}{2V}(V_o-V)] + \frac{\gamma_s(V)}{V}\Big[E(T,V) - E_{oH}\Big] \\ + \left[\frac{\Gamma(T,V) - \gamma_s(V)}{V}\right]\Big[E(T,V) - E_o(V)\Big] \end{aligned} \tag{10}$$

where E_{oH} is the energy at the foot of the Hugoniot.

P(T,V) is then written as the sum of two parts

$$P(T,V) = P_G(V,E) + P_C(T,V), \tag{11}$$

where

$$P_G(V,E) = P_H(V)\left[1 - \frac{\gamma_s(V)}{2V}(V_o - V)\right] + \frac{\gamma_s(V)}{V}\left[E(T,V) - E_{oH}\right] \tag{12}$$

is a Gruneisen-like equation of state for the solid, and

$$P_C(T,V) = \left[\frac{\Gamma(T,V) - \gamma_s(V)}{V}\right]\left[E(T,V) - E_o(V)\right] \tag{13}$$

is a correction term.

Since the EOS is referenced to the experimental Hugoniot, an explicit expression for Po(V) is not needed. However, the calculation of the temperature, as a function of energy, which is needed for the calculation of P_c requires a knowledge of $E_o(V)$. This is given by Royce[1] to be

$$E_o = \frac{C^2 - x^2}{2(1 - Sx)}\left[S + \frac{S}{3}x + \frac{S^2}{6}\left(1 - \frac{\gamma_o}{S}\right)x^2\right] + E_{oo}(1 + \gamma_o x) + E_{oH} \tag{14}$$

which he estimates to be correct to ±10 percent for compressions up to 2.

B. Melt and Liquid Regions

The Grover *liquid-metal* EOS is based on the observation that the entropy of melting can be scaled on the atomic weight using a single constant (2.32 cal/g-atom deg) for all metals and that the liquid specific heat has a universal dependence on the scaled temperature (T/T_m). These observations are supported by experimental data. Finally, the Lindemann law is used to establish the volume dependence of the melting temperature.

In BRLGRAY the fluid specific heat has a universal hyperbolic dependence on the scaled temperature:

$$C_V = \frac{3R}{2}\left\{1 + \left[\alpha\frac{T}{T_m} + 1\right]^{-1}\right\}, \quad \alpha = 0.1, \ T > T_m \tag{15}$$

This is illustrated in Figure 3, along with the Grover original linear specific heat for the liquid. The Wray form limits asymptotically to the ideal gas value.

The entropy in the liquid region is obtained from the thermodynamic relation

$$\left.\frac{\partial S}{\partial T}\right|_V = \frac{C_V}{T},$$

Using Equation 5 and integrating Equation 6 with respect to temperature gives, following Wray's notation,

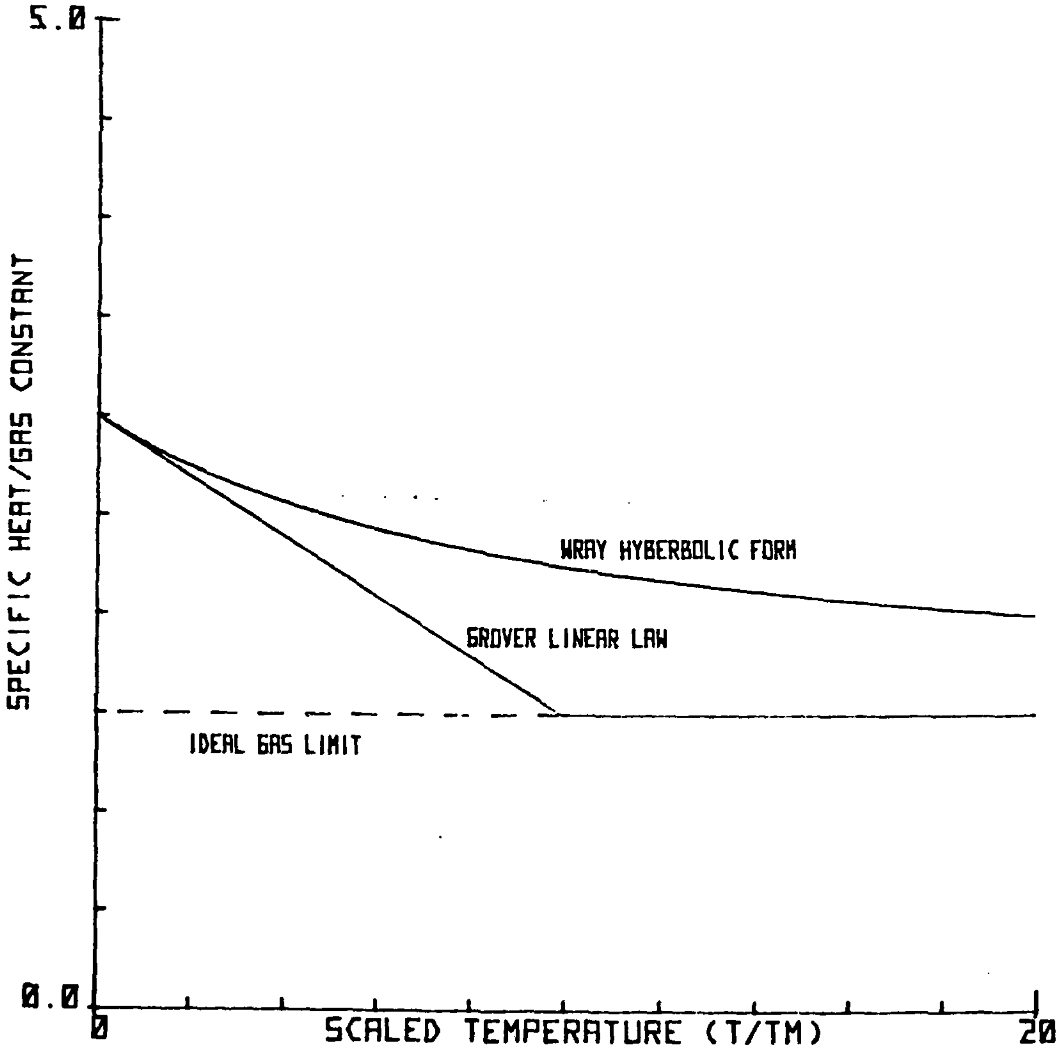

FIGURE 3. COMPARISON OF SPECIFIC HEAT FORMS

$$S_l = 3R\ln T - \frac{3R}{2}\ln\left[\alpha\frac{T}{T_m} + 1\right] + f(V)$$

Similarly for the solid,

$$S_s = 3R\ln T + h(V),$$

where f and h are undetermined functions of volume. The entropy of melting is then defined as

$$\Delta S = f(V) - h(V),$$

where ΔS is determined from experimental data[2].

The entropy in the liquid is then

$$S_l = S_s - \frac{3R}{2}\ln\left[\alpha\frac{T}{T_m} + 1\right] + \Delta S.$$

In the two-phase melt region,

$$S_m = \nu S_l + (1-\nu)S_s$$

where

$$\nu = \frac{T - T_s(V)}{T_l(V) - T_s(V)}, \quad \text{and } T_m = \frac{T_s + T_l}{2}$$

Since, in the melt region, $T \approx Tm$, the melt entropy is approximated by

$$S_m = S_s + \nu\left[\Delta S - .143R\right]. \tag{16}$$

The Helmholtz free energy A is obtained from the thermodynamic relation

$$S = -\left(\frac{\partial A}{\partial T}\right)_V,$$

which may be integrated to give

$$A = E_0(V) - \int S dT,$$

where $Eo(V)$ is the cold compression energy. This yields, after substitution and integration,

$$A_m = A_s = \nu^2(\Delta T/2)(\Delta S - .143R), \tag{17}$$

where $\Delta T = T_l(V) - T_s(V)$ and from $A = E - TS$ it follows that

$$E_m = E_s + \nu[T - \nu(\Delta T/2)](\Delta S - .143R), \tag{18}$$

where $E_s = A_s + TS_s$ is the extrapolated energy in the solid.

The pressure in the melt region is obtained by applying the relation

$$P = -\left(\frac{\partial A}{\partial V}\right)_T$$

to Equation 17, and using the approximations

$$\frac{d(\Delta T)}{dV} = 0, \quad \frac{dT_s}{dV} \approx \frac{dT_m}{dV}$$

along with the volume dependence of the melt temperature, given by the Lindemann law,

$$\lambda = \frac{-d(\ln T_m)}{d\ln V}$$

to get

$$P_m = P_s + \nu\frac{\lambda T_m}{V}(\Delta S - .143R). \tag{19}$$

The same procedure, starting with the entropy in the liquid region yields similar equations for the liquid region. These are:

$$S_l = S_s - \frac{3R}{2}\ln\left[\frac{\alpha T}{T_m} + 1\right] + \Delta S; \tag{20}$$

$$\begin{aligned} A_l = A_s &- \frac{\Delta T}{2}(\Delta S - .143R) - (T - T_m)\left[\Delta S + \frac{3R}{2}\right] \\ &+ \frac{3RT_m}{2\alpha}\left\{\left[\frac{\alpha T}{T_m} + 1\right]\ln\left[\frac{\alpha T}{T_m} + 1\right] - (\alpha + 1)\ln(\alpha + 1)\right\}; \end{aligned} \tag{21}$$

$$\begin{aligned} E_l = E_s &+ T_m\Delta S + .143R\frac{\Delta T}{2} \\ &+ \frac{3RT_m}{2\alpha}\left\{\ln\left[\alpha\frac{T}{T_m} + 1\right] - (\alpha + 1)\ln(\alpha + 1) - \left[\alpha\frac{T}{T_m} - 1\right]\right\}; \text{and} \end{aligned} \tag{22}$$

$$\begin{aligned} P_l = P_s &- \frac{\lambda T_m}{V}\Delta S \\ &- \frac{3R\lambda}{2\alpha}\frac{T_m}{V}\left\{\ln\left[\alpha\frac{T}{T_m} + 1\right] - (\alpha+1)\ln(\alpha+1) - \left[\alpha\frac{T}{T_m} - 1\right]\right\}. \end{aligned} \tag{23}$$

All of these equations are listed for reference in Appendix B.

C. The Vapor Region

The classical van der Waals equation of state has the form

$$P_v = \frac{RT}{V-V_b} - \frac{a}{V^2},$$

where a is the coefficient of attractive potential, and V_b is the hard sphere excluded volume which represents the repulsive potential by increasing the pressure at small volumes. The Young-Alder modified form of the van der Waals EOS has the form

$$P_v = \frac{RT}{V}\left[\frac{1+\eta+\eta^2-\eta^3}{(1-\eta)^3}\right] - \frac{a}{V^2}, \qquad (24)$$

where $\eta = \frac{V_b}{V}$.

The first term in Equation 24 is an algebraic approximation[14] to the hard sphere pressure, which was developed from an analysis[15] of the reduced virial series, and has been shown to describe rigid-sphere behaviour better than any other existing form.

An ideal gas caloric equation of state:

$$E_v = \frac{3RT}{2} - \frac{a}{V}$$

completed the model.

Wray[6] noted that the Gruneisen coefficient,

$$G = \frac{2}{3}\left[\frac{1+\eta+\eta^2-\eta^3}{(1-\eta)^3}\right]$$

in the Young-Alder model yielded an unreasonably high value at the join volume between the Grover and Young-Alder models, and being independent of temperature did not limit properly as temperature approached infinity. His soft-sphere model allows V_b to vary as a function of temperature, such that

$$V_b = V_b(T), \qquad \lim_{T\to\infty} V_b = 0, \qquad \lim_{T\to\infty} \frac{dV_b}{dT} = 0$$

thus yielding the correct ideal gas, high temperature limit of $G=2/3$.

---

[14] *N. F. Carnahan and K. E. Starling, Journal of Chemical Physics, 51, 635, 1969.*

[15] *B. J. Alder and T. E. Wainwright, Journal of Chemical Physics, 33, 1439, 1960.*

The generalized Rowlinson method[16] was used to relate the temperature dependence of the sphere diameter to realistic fluid behaviour, so the soft sphere diameter is calculated according to

$$d = \int_0^\infty \left[1 - e^{\frac{-u(r)}{kT}} \right] dr,$$

where u(r) is the repulsive potential. Since Grover showed his liquid scaling law to be in close agreement with computer experiments in the liquid phase for particles having an inverse-twelve potential, the following potential is used,

$$u(r) = \epsilon \left(\frac{\sigma}{r} \right)^{12}$$

where ϵ is the Fermi energy, and σ is the hard-sphere diameter. This yields, eventually,

$$d = 1.0556 \left[\frac{\epsilon \sigma^{12}}{kT} \right]^{1/12}$$

for the soft-sphere diameter.

Using the appropriate thermodynamic relations, the thermal energy E and the Helmholtz free energy A can be derived as

$$E_v = \frac{3RT}{2} - \frac{2RT^2}{V} \frac{(2-\eta)}{(1-\eta)^3} \frac{dV_b}{dT} - \frac{a}{V} + E_s \qquad (25)$$

and

$$A_v = \left[\frac{7-6\eta+\eta^2}{2(1-\eta)^3} - \ln V \right] RT - \frac{3RT}{2} \ln T - \frac{a}{V} + E_s \qquad (26)$$

The complete vapor EOS for BRLGRAY is listed in Appendix B.

D. Join Region

In Wray's join region, between the liquid and vapor states, a trigonometric mixing function was applied to the Helmholtz free energy calculated in each of the two states. All other functions of interest were then obtained through the application of the

---

[16] *H. L. Anderson, J. D. Weeks and D. Chandler, "Relationship between the Hard-Sphere Fluid and Fluids with Realistic Repulsive Forces", Physical Review, Vol. 4, No. 4, October 1971.*

appropriate thermodynamic relations. However, this method is replaced in BRLGRAY with a simple volume weighted interpolation scheme which gives better join region pressures by avoiding less accurately calculated functions in the join region.

3. EQUATION OF STATE INPUT PARAMETERS

The EOS input parameters are stored in a two-dimensional array, ESTCON(I,N), where I is the parameter index and N is the material index. This array is defined in Table 1. Table 2 lists the ESTCON data for the metals Al, Cu, and Fe. It should be noted that V_1 and V_2 in the ESTCON array (I=14 and I=15) are defined in the BRLGRAY EOS and represent the volume limits of the new join region. They replace the single join volume, Vj(I=25), of the original GRAY EOS.

The ESTCON array is maintained in data statements in a subroutine named ESTKON. Note that λ_e has the constant value .6667 for all metals and ΔS has the constant value 9.637E-05 for all metals.

TABLE 1
ESTCON PARAMETERS

Index	Symbol	Definition
1	ρ_o	Normal density Kg/m^3
2-5		Unused
6	C_o	Bulk Sound Speed (cm/s)
7	AMU	Shear Modulus (d/cm^2)
8	Y_o	Yield Strength (d/cm^2)
9	σ	Spall Strength (d/cm^2)
10	E_s	Sublimation Energy (erg/g)
11	E_{LV}	Incipient Vaporization Energy (erg/g)
12	E_{LM}	Complete Melt Energy (erg/g)
13	E_{SM}	Incipient Melt Energy (erg/g)
14	V_1	Liquid-Join Boundary (m^3/Kg)
15	V_2	Join-Vapor Boundary (m^3/Kg)
16	S	Hugoniot Parameter: (cm/μsec)
17	λ_o	Lattice gamma:$\lambda(V)=\lambda_o-ax$
18	a	Defined in ESTCON(17,N)
19	λ_e	Electronic gamma
20	g_e	Electronic energy coefficient (mbar cm^3/mole deg^2)
21	T_{MO}	Melt temperature (°K) at $V=V_o$
22	E_{oH}	Energy at $V=V_o$,$T=300$°K, $P=0$,(mbar cm^2/g)
23	E_∞	Energy difference between E_{oH} and energy at $V=V_o$,$T=0$(mbar cm^3/g) Default value: $E_\infty=-300(3*8.134*10^{-5}+150g_e)/W$
24	W	Atomic weight (g/mole)
25		Unused
26	V_b	Vapor exclusion volume (m^3/Kg)
27	a_Y	Coefficient of attractive potential mbar(cm^3/mole)^2
28	T_c	Critical temperature (°K)
29	ΔS	Entropy of melting mbarcm^3/mole°)
30	EOSFLG	Equation of state flag

TABLE 2

ESTCON DATA

Symbol	Al	Cu	Fe
ρ_o	2.7	8.94	7.87
C_o	5.44E+05	3.94E+05	5.13E+05
E_s	1.18E+11	5.37E+10	6.80E+10
E_{LV}	2.65E+10	4.79E+10	--------
E_{LM}	1.06E+10	6.67E+09	1.49E+10
E_{SM}	6.62E+09	4.62E+09	1.16E+10
V_1	.40	.12	.14
V_2	.58	.16	.18
S	1.34	1.49	1.40
λ_o	2.18	1.97	1.80
a	1.70	1.50	1.50
λ_e	.6667	.6667	.6667
g_e	8.70E-09	4.90E-09	9.60E-09
T_{M0}	1220	1790	2385
W	26.98	63.54	55.85
V_b	.190	.056	.066
a_Y	47.0	35.0	31.0
T_c	10633	11407	9753

4. THE DATGEN PROGRAM

In order to use the BRLGRAY EOS in the liquid-vapor, mixed-phase region it is necessary to calculate the four critical constants:

V_c, T_c, and $P_c(V_c,T_c)$ and $E_c(V_c,T_c)$,

and the mixed-phase boundary. We calculate these using a program which is based on the main subroutine given by Young[5] .

Initially the critical volume is estimated to be 4.35 times the boiling point volume. An iteration process, using pressures P(V,T), generated by the EOS, then locates the critical isotherm and the volume for which $\Delta P/\Delta V$ is zero on the critical isotherm, the critical volume. At this point $P=P_c$ and E_c is calculated by the EOS. The code then chooses a set of equally spaced temperatures between T_c and T_{mo}, the melting temperature parameter, to draw tie lines connecting the high density liquid with the low density vapor. The corresponding pressures and equilibrium liquid and vapor densities are computed by Maxwell construction. The locus of these tie-line end points then forms the dome-shaped, mixed-phase boundary in PV space. The corresponding energies $E(V_{min},T)$ and $E(V_{max},T)$ are also computed for each temperature and the data is stored in a permanent file for access by the EOS. The associated variable names are:

TMP:temperature on a tie line	(°K)
VMN:volume on liquid end of tie line	(m^3/Mg)
VMX:volume on vapor end of tie line	(m^3/Mg)
EVMN:energy at VMN and TMP	(erg/g)
EVMX:energy at VMX and TMP	(erg/g)
PRES:pressure on a tie line	(d/cm^2)

where d/cm^2 are working units in the code, and are equivalent to 10^{-1} Pascals.

The DATGEN program also has an isotherm driver subroutine which generates isotherms in P-V space using the EOS along with subroutine ET[5]. Subroutine ET calculates the specific internal energy consistent with the driver values of specific volume and temperature. The BRLGRAY EOS is then called to calculate the pressure. This program is used to determine the volume limits of the new join region in BRLGRAY. Wray[6] performed such calculations for three metals: Al, Fe, and U. We have made calculations for seventeen materials using slightly different procedures, and in this report have presented data for Al, Fe, and Cu. These calculations are described in the next section of this report.

5. MIXED-PHASE DATA GENERATION

Figure 4 shows a P-V plot of the regions defined in BRLGRAY. Pressure and temperature from the liquid and vapor phases are volume weighted in the join region.

Figure 5 shows a schematic diagram of representative isotherms in the join region. The values of V_1 and V_2 are chosen such that pressure maxima and minima do not occur along an isotherm in the join region. Such constructs would make it impossible for the DATGEN program to find the critical isotherm in subsequent mixed-phase boundary calculations.

Wray used a trial and error procedure in which isotherms were generated for various values of V_1 and V_2. We used a similar isotherm driver but ran separate cases in which the EOS was constrained to either the solid-liquid or the vapor model. Analysis of these pressure isotherms then allowed a good initial estimate of V_1 and V_2.

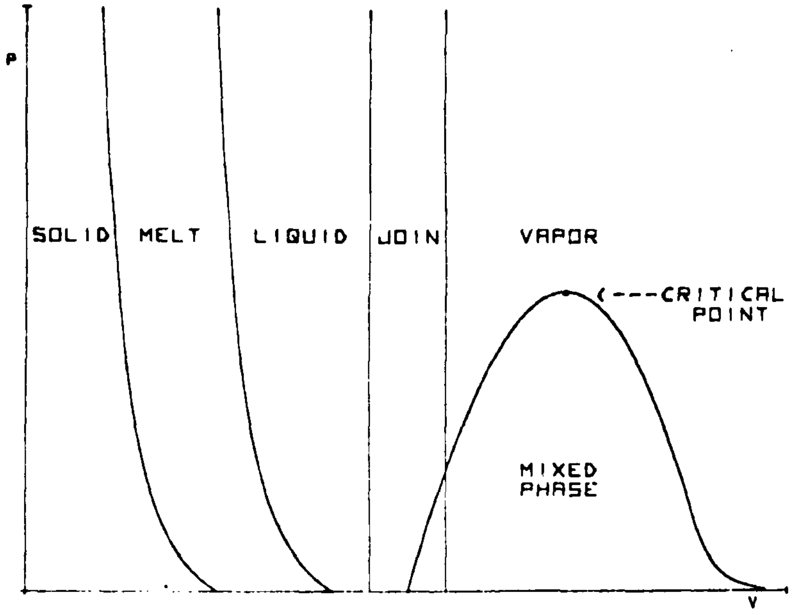

FIGURE 4 SCHEMATIC PHASE DIAGRAM FOR BALGRAY

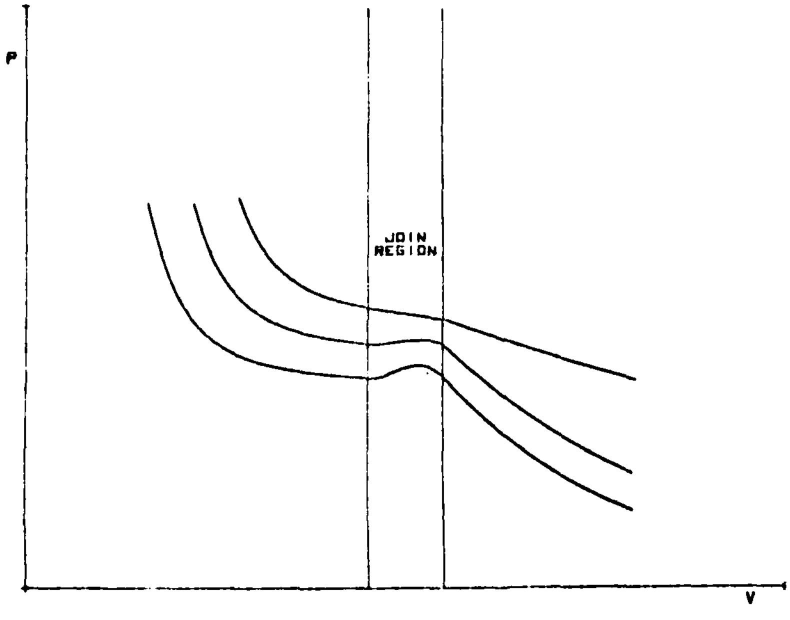

FIGURE 5 SCHEMATIC DIAGRAM OF BALGRAY ISOTHERMS

The isotherms generated by the solid-liquid model were well behaved up to a volume at which the model failed catastrophically. These isotherms gave a good indication of the maximum value which V_1 could take. Comparison of these isotherms with isotherms generated by the vapor model then allowed an estimate of the best value of V_2.

Isotherms generated using these values of V_1 and V_2 generally gave positive pressures in the join region, without maxima or minima, for the temperatures of interest.

Alternatively, once these parameters have been generated for a number of metals one may estimate V_1 and V_2 for a new metal using the following scaling rule:

$$\rho_o V_1 = 1.1 = C_1$$

$$\rho_o V_2 = 1.4 = C_2$$

where the C_i are average values of $\rho_o V_i$. The V_i estimated in this way will need very little adjustment after observation of the isotherms in the join region using the complete EOS.

The driver routine was programmed to generate isotherms which ranged from 20,000°K down to 2,000°K in decrements of 2,000°K, and to lower temperatures in smaller steps. Volumes ranged from .01 m^3/Mg to beyond the mixed-phase region in equal increments of ln V.

Aluminum isotherms were generated starting with a specific volume of .01 and incremented until the calculation failed. Inspection of the code output then determined maximum values of V_1 for each isotherm. These values, shown in Table 3, ranged from .67 m^3/Mg at 20,000°K to .37 m^3/Mg at 300°K. In anticipation of being able to extend the validity of the model to below 1,000°K, at these volumes, we chose V_1 to be 40 m^3/Mg.

Vapor-model aluminum isotherms were then generated starting with specific volumes equal to .355 m^3/Mg and extending beyond the expected value of V_2. Comparison of these isotherms with those generated with the solid-liquid model showed a crossover point for each isotherm which was taken as the minimum value of V_2 in each case. These values, shown in Table 4, ranged from .58 m^3/Mg at 20,000°K to .54 m^3/Mg at 6,000°K. Thus .58 m^3/Mg was interpreted as an upper bound on V_2, ensuring that crossover would occur, within the join region, for all temperatures below 20,000°K.

Finally, a set of isotherms were generated in the code's normal mode (in which it determines the thermodynamic phase and chooses the corresponding model of the EOS) using the values V_1=.40 m^3/Mg and V_2=.58 m^3/Mg. These isotherms gave positive pressures in the join region without maxima or minima for temperatures down to 1,000°K. A set of isotherms using V_1 = .41 m^3/Mg showed a minimum in the join region at 4,000°K, and a set using .37 m^3/Mg showing minima in the 1,000°K isotherm.

TABLE 3
V_{1max} for Aluminum Isotherms Using Solid-Liquid Model

Temperature (K)	V_{1max} (m^3/Mg)	Phase
20,000	.67	Liquid
15,000	.66	
10,000	.62	
8,000	.61	Melt
6,000	.58	Solid/Melt/Liquid
4,000	.54	
2,000	.45	
1,000	.41	
500	.37	
300	.37	

TABLE 4

V_2 min For Aluminum Isotherms Using Vapor Model

Temperature (K)	V_{2min} (m^3/Mg)	Phase
20,000	.58	Vapor
10,000	.56	
8,000	.55	
6,000	.54	

V_1 and V_2 were determined, using the same approach, for the other metals. These are shown in Table 5 along with the values for Al.

Once the volume limits of the join region were determined for each of the metals, the DATGEN program was used to calculate the critical point, and subsequently the mixed-phase boundary. Critical point data for the five metals is shown in Table 6.

Finally the DATGEN program is used to generate the mixed-phase boundaries.

This data is shown in Tables 7 - 9.

TABLE 5
JOIN VOLUMES

Metal	V_1	V_2
Al	.40	.58
Cu	.12	.16
Fe	.14	.18

TABLE 6
CRITICAL POINTS

Metal	Vc (m^3/Mg)	Tc (°K)	Pc (10^8*P)	Ec (.1mJ/g)
Al	1.460	7180	5.34E-03	1.25E+09
Cu	.413	8880	9.88E-03	6.34E+10
Fe	.498	9910	1.04E-02	7.24E+10

TABLE 7

ALUMINUM MIXED-PHASE BOUNDARY

T_c	V_c	P_c	E_c
7178	1.46	5.34E+09	1.25E+11

TMP	VMN	VMX	EVMN	EVMX	PRES
6.64E+03	8.93E-01	3.03E+00	1.07E+11	1.35E+11	3.83E+11
6.09E+03	7.63E-01	4.76E+00	9.87E+10	1.37E+11	3.83E+09
5.55E+03	6.85E-01	7.69E+00	9.16E+10	1.38E+11	1.68E+09
5.01E+03	6.33E-01	1.25E+01	8.55E+10	1.37E+11	9.98E+08
4.47E+03	5.95E-01	2.00E+01	8.01E+10	1.36E+11	5.31E+08
3.93E+03	5.68E-01	3.33E+01	7.50E+10	1.35E+11	2.40E+08
3.39E+03	5.56E-01	1.11E+02	7.01E+10	1.33E+11	8.86E+07
2.85E+03	5.46E-01	2.50E+02	6.52E+10	1.31E+11	3.21E+07
2.30E+03	5.38E-01	1.11E+03	5.81E+10	1.28E+11	5.70E+06
1.76E+03	5.10E-01	1.43E+04	4.14E+10	1.26E+11	3.64E+05
1.22E+03	4.22E-01	3.33E+06	1.40E+10	1.24E+11	9.88E+02

TABLE 8

COPPER MIXED-PHASE BOUNDARY

T_c	V_c	P_c	E_c
8492	.435	8.91E+09	6.33E+11

TMP	VMN	VMX	EVMN	EVMX	PRES
7.83E+03	2.69E-01	8.93E-01	5.49E+10	6.85E+10	6.50E+09
7.22E+03	2.31E-01	1.39E+00	5.08E+10	6.96E+10	4.55E+09
6.62E+03	2.09E-01	2.13E+00	4.74E+10	6.99E+10	3.02E+09
6.01E+03	1.93E-01	3.33E+00	4.45E+10	6.98E+10	1.87E+09
5.41E+03	1.81E-01	5.55E+00	4.18E+10	6.93E+10	1.05E+09
4.81E+03	1.72E-01	1.00E+01	3.94E+10	6.86E+10	5.23E+08
4.20E+03	1.65E-01	2.00E+01	3.73E+10	6.78E+10	2.17E+08
3.60E+03	1.59E-01	5.00E+01	3.52E+10	6.68E+10	6.93E+07
2.98E+03	1.55E-01	2.00E+02	2.94E+10	6.57E+10	1.74E+07
2.39E+03	1.49E-01	1.67E+03	2.28E+10	6.46E+10	1.83E+06
1.79E+03	1.38E-01	5.00E+04	1.33E+10	6.34E+10	3.50E+04

TABLE 9

IRON MIXED-PHASE BOUNDARY

T_c	V_c	P_c	E_c
9913	.498	1.04E+10	7.23E+10

TMP	VMN	VMX	EVMN	EVMX	PRES
9.23E+03	3.12E-01	1.01E+00	6.15E+10	7.94E+10	7.69E+09
8.54E+03	2.67E-01	1.54E+00	5.60E+10	8.08E+10	5.46E+09
7.86E+03	2.41E-01	2.33E+00	5.16E+10	8.13E+10	3.70E+09
7.18E+03	2.23E-01	3.57E+00	4.78E+10	8.11E+10	2.35E+09
6.49E+03	2.09E-01	5.88E+00	4.43E+10	8.06E+10	1.38E+09
5.81E+03	1.99E-01	1.00E+01	4.11E+10	7.98E+10	7.20E+08
5.12E+03	1.90E-01	2.00E+01	3.82E+10	7.87E+10	3.24E+08
4.44E+03	1.83E-01	5.00E+01	3.36E+10	7.75E+10	1.14E+08
3.75E+03	1.73E-01	1.67E+02	2.63E+10	7.61E+10	3.14E+07
3.07E+03	1.49E-01	1.11E+03	1.76E+10	7.47E+10	3.83E+06
2.39E+03	1.43E-01	2.00E+04	1.36E+10	7.32E+10	1.43E+05

6. Conclusion

Equation-of-state input parameters have been generated for seventeen different materials. Data has been shown here for Al, Cu, and Fe. The EOS has been installed in the BRLHELP code and comparisons have been made with the Tillotson EOS and the temperature fit in the HULL code. In the solid state the agreement between BRLGRAY, Tillotson, the HULL EOS's, and with experimental data is excellent. Significantly, BRLGRAY uses no more computer time for the solid state than do the other EOS's, while outperforming them in calculating phase change phenomena.

The BRLGRAY EOS is being made available for use by hydrocode users at the BRL and at the ARC computers at Huntsville, as part of the BRLEOS code system[17].

---

[17] *Joseph Lacetera and W. Buchheister, "BRLPUFF and the BRLEOS Code System" BRL IMR No. 655, Aug 1979.*

REFERENCES

1. E.B. Royce, "GRAY, A Three-Phase Equation of State for Metals", Lawrence Livermore Laboratory, UCRL-51121, Sep 1971.

2. R. N. Keeler and E. B. Royce, "Shock Waves in Condensed Media", Lawrence Livermore Laboratory, UCRL-71846, 1969.

3. R. Grover, "Liquid Metal Equation of State Based on Scaling", J. Chem Phys, 55, 3435, 1971.

4. D. A. Young and B. J. Alder, "Critical Point of Metals from the van der Waals Model", Phys Rev A3, 364, 1971.

5. D. A. Young, "Modification of the GRAY Equation of State in the Liquid-Vapor Region", Lawrence Livermore Laboratory, UCRL-51575, Apr 15, 1974.

6. William O. Wray and Robert A. Cecil, "Modified GRAY: An Improved Three-Phase Equation of State for Metals". BRL CR No. 299, April 1976. (AD #A025260)

7. J. H. Tillotson, "Metal Equations of State for Hypervelocity Impact", General Atomic Report GA-3216, July 1962.

8. Laura J. Hageman, et al., "HELP, A Multi-Material Eulerian Program for Compressible Fluid and Elastic-Plastic FLows in Two Space Dimensions and Time", Systems, Science and Software Report TR-76-45-BK2, April 1976.

9. Richard E. Durrett and David A. Matuska, "The HULL Code, A Finite Difference Solution to the Equations of Continuum Mechanics", Air Force Armament Laboratory, AFATL-TR-78-125, November, 1978.

10. J. Lacetera, J. E. Lacetera, and J. A. Schmitt, "The BRL 7600 Version of the HELP Code", BRL REPORT ARBRL-TR-02209, Jan 80. (AD #A082804)

11. J. A. Schmitt, "An Improved Internal Energy Calculation for the HELP Code and Its Implications to Conical Shaped Charge Simulations", BRL Report ARBRL-TR-02168, Jun 79. (AD #A072785)

12. J. Lacetera, "BRLHELP80: NAMELIST INPUT", BRL IMR No 677, Mar 80.

13. Janet Lacetera, "Study of Liner Collapse and Jet Formation for Various Hemispherical Shaped-Charge Designs", BRL Draft Report.

14. N. F. Carnahan and K. E. Starling, Journal of Chemical Physics, 51, 635, 1969.

15. B. J. Alder and T. E. Wainwright, Journal of Chemical Physics, 33, 1439, 1960.

16. H. L. Anderson, J. D. Weeks and D. Chandler, "Relationship between the Hard-Sphere Fluid and Fluids with Realistic Repulsive Forces", Physical Review, Vol. 4, No. 4, October 1971.

17. Joseph Lacetera and W. Buchheister, "BRLPUFF and the BRLEOS Code System" BRL IMR No. 655, Aug 1979.

APPENDIX A

All symbols used in this report are defined where they first appear in the text. However, selected symbols are listed here for convenience.

(A-1)	$R' = R/W$	atomic weight scaled gas constant
(A-2)	$G' = g_e /W$	atomic weight scaled electronic energy coefficient
(A-3)	$\gamma_s(V)$	volume dependent Gruneisen coefficient for solid
(A-4)	γ_e	electronic gamma (normally 2/3)
(A-5)	W	atomic weight
(A-6)	N_e	number of free electrons
(A-7)	U_s	shock velocity
(A-8)	U_p	particle velocity
(A-9)	C	U_s intercept at zero pressure
(A-10)	S	slope of shock/particle velocity data
(A-11)	$x = \frac{V_o - V}{V}$	compression variable
(A-12)	E_{0H}	Energy at $V=V_o$, $T=300°K$, $P=0$
(A-13)	E_∞	Energy difference between E_{oH} and energy at $V=V_o$, $T=0$ Default$= -300(3*8.134*10^{-5}+150g_e)/W$
(A-14)	α	constant in hyperbolic form of specific heat
(A-15)	ΔS	constant entropy of melting constant$=9.62*10^{-5}$ Mbar $cm^3/mole^o$
(A-16)	T_m	melting temperature (°K)

APPENDIX B

$$E_s(T,V) = E_o(V) + 3R' + \frac{G'T^2}{2} \tag{1}$$

$$P_s(T,V) = P_o(V) + 3\gamma_s(V)\frac{R'T}{V} + \frac{1}{2}\gamma_e\frac{G'T^2}{V} \tag{2}$$

$$G' = \frac{\pi^2 N_e k R'}{2E_f} \tag{3}$$

$$E_f = 26\left[\frac{N_e}{WV_o}\right]^{2/3} \tag{4}$$

$$U_s = C + SU_p \tag{5}$$

$$P_H(V) = \frac{\rho_o C^2 x}{(1-Sx)^2} \tag{6}$$

$$E_H(V) = \frac{1}{2}P_H(V)[V_o - V] + E_{oH} \tag{7}$$

$$P(T,V) = P_o(V) + \frac{\Gamma(T,V)}{V}\Big[E(T,V) - E_o(V)\Big] \tag{8}$$

$$P_H = P_o(V) + \frac{\gamma_s(V)}{V}\Big[E_H(V) - E_o(V)\Big] \tag{9}$$

$$\begin{aligned} P(T,V) = {} & P_H(V)[1 - \frac{\gamma_s(V)}{2V}(V_o - V)] + \frac{\gamma_s(V)}{V}\Big[E(T,V) - E_{oH}\Big] \\ & + \left[\frac{\Gamma(T,V) - \gamma_s(V)}{V}\right]\Big[E(T,V) - E_o(V)\Big] \end{aligned} \tag{10}$$

$$P(T,V) = P_G(V,E) + P_C(T,V) \tag{11}$$

$$P_G(V,E) = P_H(V)\left[1 - \frac{\gamma_s(V)}{2V}(V_o - V)\right] + \frac{\gamma_s(V)}{V}\Big[E(T,V) - E_{oH}\Big] \tag{12}$$

$$P_C(T,V) = \left[\frac{\Gamma(T,V) - \gamma_s(V)}{V}\right]\left[E(T,V) - E_o(V)\right] \tag{13}$$

$$E_o = \frac{C^2 - x^2}{2(1-Sx)}\left[S + \frac{S}{3}x + \frac{S^2}{6}(1-\frac{\gamma_o}{S})x^2\right] + E_{oo}(1+\gamma_o x) + E_{oH} \tag{14}$$

$$C_V = \frac{3R}{2}\left\{1 + \left[\alpha\frac{T}{T_m} + 1\right]^{-1}\right\}, \qquad \alpha = .1,\ T > T_m \tag{15}$$

$$S_m = S_s + \nu\left\{\Delta S - .143R\right\} \tag{16}$$

$$A_m = A_s = \nu^2(\Delta T/2)(\Delta S - .143R) \tag{17}$$

$$E_m = E_s + \nu[T - \nu(\Delta T/2)](\Delta S - .143R) \tag{18}$$

$$P_m = P_s + \nu\frac{\lambda T_m}{V}(\Delta S - .143R) \tag{19}$$

$$S_l = S_s - \frac{3R}{2}\ln\left[\frac{\alpha T}{T_m} + 1\right] + \Delta S \tag{20}$$

$$\begin{aligned} A_l = A_s &- \frac{\Delta T}{2}(\Delta S - .143R) - (T - T_m)\left[\Delta S + \frac{3R}{2}\right] \\ &+ \frac{3RT_m}{2\alpha}\left\{\left[\frac{\alpha T}{T_m} + 1\right]\ln\left[\frac{\alpha T}{T_m} + 1\right] - (\alpha + 1)\ln(\alpha + 1)\right\} \end{aligned} \tag{21}$$

$$\begin{aligned} E_l = E_s &+ T_m\Delta S + .143R\frac{\Delta T}{2} \\ &+ \frac{3RT_m}{2\alpha}\left\{\ln\left[\alpha\frac{T}{T_m} + 1\right] - (\alpha + 1)\ln(\alpha + 1) - \left[\alpha\frac{T}{T_m} - 1\right]\right\} \end{aligned} \tag{22}$$

$$\begin{aligned} P_l = P_s &- \frac{\lambda T_m}{V}\Delta S \\ &- \frac{3R\lambda}{2\alpha}\frac{T_m}{V}\left\{\ln\left[\alpha\frac{T}{T_m} + 1\right] - (\alpha+1)\ln(\alpha+1) - \left[\alpha\frac{T}{T_m} - 1\right]\right\} \end{aligned} \tag{23}$$

$$P_v = \frac{RT}{V}\left[\frac{1+\eta+\eta^2-\eta^3}{(1-\eta)^3}\right] - \frac{a}{V^2} \tag{24}$$

$$E_v = \frac{3RT}{2} - \frac{2RT^2}{V}\frac{(2-\eta)}{(1-\eta)^3}\frac{dV_b}{dT} - \frac{a}{V} + E_s \tag{25}$$

$$A_v = \left[\frac{7-6\eta+\eta^2}{2(1-\eta)^3} - \ln V\right] RT - \frac{3RT}{2}\ln T - \frac{a}{V} + E_s \tag{26}$$

DISTRIBUTION LIST

No. of Copies	Organization
12	Commander Defense Technical Info Center ATTN: DDC-DDA Cameron Station Alexandria, VA 22314
1	Director Defense Advanced Research Projects Agency Tactical Technical Office ATTN: Dr. James Tegnelia 1400 Wilson Boulevard Arlington, VA 22209
1	Director Institute for Defense Analysis ATTN: Dr. Bruce J. Whittemore 400 Army Navy Drive Arlington, VA 22202
1	Deputy Under Secretary of the Army for Operations Research ATTN: Mr. David Hardison Washington, DC 20310
1	Commander US Army Materiel Development and Readiness Command ATTN: DRCDMD-ST 5001 Eisenhower Avenue Alexandria, VA 22333
2	Commander US Army Armament Research and Development Command ATTN: DRDAR-TSS Dover, NJ 07801
1	Commander US Army Armament Research and Development Command ATTN: DRDAR-LCA-L, Mr. G. Randers-Pehrson Dover, NJ 07801
1	Commander US Army ARRADCOM Benet Weapons Laboratory ATTN: DRDAR-LCB-TL Watervliet, NY 12189
1	Commander US Army Armament Materiel Readiness Command ATTN: DRSAR-LEP-L, Tech Lib Rock Island, IL 61299
1	Commander US Army Aviation Research and Development Command ATTN: DRSAV-E P.O. Box 209 St. Louis, MO 63166
1	Director US Army Air Mobility Research and Development Laboratory Ames Research Center Moffett Field, CA 94035
1	Commander US Army Communications Rsch and Development Command ATTN: DRDCO-PPA-SA Fort Monmouth, NJ 07703
1	Commander US Army Electronics Research and Development Command Technical Support Activity ATTN: DELSD-L Fort Monmouth, NJ 07703
2	Commander US Army Missile Command ATTN: DRSMI-R DRSMI-YDL Redstone Arsenal, AL 35809

DISTRIBUTION LIST

No. of
Copies Organization

1 Commander
US Army Tank Automotive
Research & Development Command
ATTN: DRDTA-UL
Warren, MI 48090

1 Commander
US Army Materials and
Mechanics Research Center
ATTN: DRXMR-T, Mr. J. Mescall
Watertown, MA 02172

1 Director
US Army TRADOC Systems
Analysis Activity
ATTN: ATAA-SL, Tech Lib
White Sands Missile Range,
NM 88002

1 AFATL/DLJW/CPT Raymond Bell
Eglin AFB, FL 32542

2 Director
Lawrence Radiation Laboratory
ATTN: Dr. David Young
Dr. Richard Grover
P.O. Box 808
Livermore, CA 94550

1 Science Applications, Inc.
ATTN: Mr. Ken Dent
2019 W. Clinton Avenue
Suite 800
Huntsville, AL 35805

1 University of California
Los Alamos Scientific Lab
ATTN: Dr. R. Karpp
P.O. Box 1663
Los Alamos, NM 87545

Aberdeen Proving Ground

Dir, USAMSAA
ATTN: DRXSY-D
DRXSY-MP, H. Cohen
Cdr, USATECOM
ATTN: DRSTE-TO-F
Dir, USA CSL, Bldg. E3516
ATTN: DRDAR-CLB-PA

USER EVALUATION OF REPORT

Please take a few minutes to answer the questions below; tear out this sheet and return it to Director, US Army Ballistic Research Laboratory, ARRADCOM, ATTN: DRDAR-TSB, Aberdeen Proving Ground, Maryland 21005. Your comments will provide us with information for improving future reports.

1. BRL Report Number ________________________

2. Does this report satisfy a need? (Comment on purpose, related project, or other area of interest for which report will be used.)

____

____

____

3. How, specifically, is the report being used? (Information source, design data or procedure, management procedure, source of ideas, etc.) ________________________

____

____

4. Has the information in this report led to any quantitative savings as far as man-hours/contract dollars saved, operating costs avoided, efficiencies achieved, etc.? If so, please elaborate.

____

____

5. General Comments (Indicate what you think should be changed to make this report and future reports of this type more responsive to your needs, more usable, improve readability, etc.) ____________

____

____

____

6. If you would like to be contacted by the personnel who prepared this report to raise specific questions or discuss the topic, please fill in the following information.

Name: ________________________

Telephone Number: ________________________

Organization Address: ________________________

____

____